Online Journal of Art and Design
volume 15, issue 1, January 2027
DOI: https://doi.org/10.30935/ojad/2513146

Assessment of Neighborhood Urban Heat Island Resilience through Urban Fabric and Socio-economic Capacity: A Case Study on LCZ 2 Neighborhoods in Konya, Türkiye

Gizem Derinci Alper
Konya Technical University, Faculty of Architecture and Design, City and Regional Planning, Konya, Turkiye
gderinci@ktun.edu.tr
ORCID: https://orcid.org/0000-0003-2393-6269

Kadriye (Deniz) Topçu
Konya Technical University, Faculty of Architecture and Design, City and Regional Planning, Konya, Turkiye
ktopcu@ktun.edu.tr
ORCID: https://orcid.org/0000-0003-4530-1969

"This article is derived from the pilot study conducted within the scope of the author's ongoing PhD dissertation entitled "Evaluation of Urban Fabrics in the Context of Urban Resilience towards Climate Change."

Abstract
Local Climate Zones (LCZs) provide an important framework for classifying the physical and thermal characteristics of urban areas, but they are limited in explaining the socio-economic and urban morphological differences of neighborhoods within the same LCZ class. This study aims to examine whether urban heat resilience differs in terms of socio-economic and urban fabric characteristics in neighborhoods within the same LCZ class. Accordingly, nine neighborhoods in Konya, Türkiye, classified under LCZ 2, were comparatively analyzed under low, medium, and high socio-economic capacity groups. In this study, urban heat resilience was evaluated within the framework of exposure, sensitivity, and adaptive capacity components. The climatic, socio-economic, and urban fabric indicators representing these components were normalized to create the Neighborhood Heat Resilience Index. The findings reveal substantial differences among neighborhoods within the same LCZ 2 class in terms of land surface temperature, urban fabric characteristics, and socio-economic conditions, as well as in their overall resilience scores. Neighborhoods with higher socio-economic capacity generally exhibited higher adaptive capacity scores. Furthermore, high land surface temperature alone did not necessarily correspond to low overall resilience, highlighting the importance of jointly assessing thermal conditions, urban fabric characteristics, and socio-economic capacity to understand neighborhood-level heat resilience.
Keywords: Local climate zone, neighborhood climate resilience, socio-economic capacity, urban fabric, urban heat island (UHI), land surface temperature (LST)

1. INTRODUCTION

Today, cities have become spatial systems characterized by the intensive consumption of energy and natural resources on a global scale, resulting in significant environmental impacts. The fact that 75% of energy consumption, 60% of residential water use, and 80% of greenhouse gas emissions occur in cities highlights the magnitude of their environmental footprint (Kennedy et al., 2011). This indicates that cities should not be viewed merely as spatial formations with increasing population and structural density; rather, they could be understood as complex ecological systems that require substantial inputs of resources and energy while simultaneously generating various forms of waste and emissions. Consequently, balancing the relationship between a city's dependence on natural resources and the pressure it exerts on environmental systems emerges as a fundamental requirement for sustainable urban development. As cities grow and evolve into increasingly complex urban systems, their demand for resources and energy rises, further intensifying their reliance on the environment. This process, which drives the need for more built environments, also heightens the vulnerability of cities to environmental changes and

various external shocks (Timmeren, 2012). In this context, urban resilience stands out in the literature as a key theoretical framework for sustainably reorganizing the relationship between the city and the natural environment, and for strengthening urban systems' capacity to maintain their functions amid changing environmental conditions.

Urban resilience implies that urban systems cannot be reduced to a single, static state of equilibrium; On the contrary, it is based on the idea that they should be approached as complex structures that are constantly changing and transforming because of the interaction between various subsystems. In this context, Eraydin and Taşan-Kok (2013) emphasize that urban resilience should be defined by examining the resilience characteristics of urban areas in conjunction with the vulnerability indicators of their constituent subsystems. Consequently, urban resilience encompasses not only the capacity of urban systems to return to their original state following an external shock, but also their ability to reduce the vulnerabilities of urban subsystems, learn and adapt to changing conditions, and—when necessary—undergo transformation (Wu and Wu, 2013). The development of these capacities is closely linked to how urban space is produced. Models of urban space production that prioritize capital maximization while disregarding long-term social and ecological issues can negatively affect urban resilience. Increased building density, the proliferation of impermeable surfaces, the loss of vegetation, and rising energy consumption significantly alter the thermal properties of cities and increase urban heat generation. This phenomenon—referred to in the literature as the "urban heat island" effect and becoming particularly pronounced during periods of high temperature—increases the urban population's exposure to heat and shifts the spatial distribution of heat-related environmental risks within the city. Urban fabric characteristics—such as building density, the geometry of buildings and plots, the spatial configuration of streets, the distribution of open and green spaces, and the ratio of permeable surfaces—play a decisive role in the formation of these thermal conditions (Ronchi et al., 2020; Erdem Okumuş and Terzi, 2021).

However, the sensitivity to temperature and the adaptive capacity of a population living within the same physical environment are not homogeneous. Factors such as income level, educational attainment, population density, and the spatial distribution of vulnerable groups (e.g., children, the elderly) shape the social dimension of temperature-related risks. Consequently, basing assessments of urban heat risk and resilience solely on physical environmental indicators may lead to the neglect of socio-economic disparities and their potential influence on temperature-related risks. To gain a more comprehensive understanding of these risks, it is essential to consider the social and economic characteristics of the population (Anguelovski et al., 2016). Therefore, urban heat resilience requires a multidimensional approach—one that goes beyond merely mapping the spatial distribution of temperature to also evaluate the interrelationships between exposure, sensitivity, and risk (IPCC, 2014). A review of the relevant literature reveals that the formation and spatial distribution of the "urban heat island" effect—a prominent climate change-related risk in cities—are assessed primarily through the lens of physical characteristics. Nevertheless, there is an increasing emphasis on the fact that factors such as the socio-economic traits of the population and the adaptive capacities of different social groups can also shape the spatial distribution of climate risks associated with urban heat. At this juncture, the Local Climate Zones (LCZ) classification system—developed by Stewart and Oke in 2012—offers a significant methodological framework that enables the establishment of a relationship between urban climate and urban morphology. By acting as a bridge that links the urban heat island effect with planning indicators (such as land cover and land use) and structural indicators (such as building density and height) across various spatial scales (Wang et al., 2024), LCZ maps create a common morphological language (Stewart, 2024). The LCZ classification comprises a total of 17 categories: 10 for built-up areas and 7 for natural environments (Oke et al., 2017).

Although the LCZ classification provides a comparable framework for urban areas in terms of structural characteristics and surface properties (Stewart and Oke, 2012), urban fabric

features—such as parcel size, building density, street openness, street network configuration, the ratio of permeable surfaces, and vegetation—can vary even among neighborhoods belonging to the same LCZ class. Such neighborhoods may exhibit significant differences in socio-economic characteristics, including population density, income levels, educational attainment, and the distribution of vulnerable population groups. Beyond the common urban fabric traits identified by the high-level LCZ classification, substantial physical and social disparities may exist at the neighborhood scale.Consequently, belonging to the same LCZ class does not imply that neighborhoods share similar characteristics regarding exposure to urban heat, vulnerability, or adaptive capacity. In this context, rather than comparing different LCZs, this study examines neighborhoods located within the same LCZ to reveal how variations in urban fabric and socio-economic capacity are reflected in the climatic resilience profiles of these neighborhoods. This raises a question within the scope of urban heat research: "Do urban fabrics situated within the same LCZ—yet possessing different socio-economic capacities—exhibit varying levels of resilience against urban heat?"

While a significant portion of existing research focuses on thermal differences between various Local Climate Zones (LCZs) or the impact of urban fabric on surface temperatures, studies conducted at the neighborhood scale—addressing socio-economic and urban fabric variations within the same LCZ class—remain quite limited. To this end, urban areas classified as LCZ 2—representing varying levels of socio-economic capacity—were examined through the lenses of urban fabric, land surface temperature, and socio-economic indicators, framed by the dimensions of resilience: exposure, sensitivity, and adaptive capacity. Consequently, integrating the comparable physical framework provided by the LCZ classification with neighborhood-scale socio-economic and structural variations will contribute to a more nuanced understanding of resilience against urban heat. The contribution of this article is to demonstrate that neighborhoods falling within the same broad morphological LCZ 2 category can exhibit distinct resilience profiles when factors such as exposure, sensitivity, and adaptive capacity are considered together.

In this context, urban areas located within the LCZ 2 category in the city of Konya, Türkiye—comprising nine neighborhoods with distinct socio-economic capacities, were selected as sample sites. In the relevant literature, among studies measuring Urban Heat Island (UHI) effects during daytime hours, the LCZ 2 class—characterized by a compact, mid-rise urban structure, is identified as the hottest zone (Rahmani and Sharafi, 2025). Selecting this class allows for the urban typology to be held relatively constant, thereby enabling an examination of the relationship between shifts in socio-economic characteristics and profiles of resilience against urban heat. Konya was selected as the study area due to several factors: the extensive geographical spread of its central districts, the presence of diverse urban fabrics and distinct socio-economic disparities, a high level of exposure to heatwaves, and a scarcity of existing research addressing this issue at the neighborhood scale. Accordingly, areas in Konya classified as "LCZ 2" were evaluated not merely as a form of urban categorization, but also within a framework that facilitates the comparison of exposure, sensitivity, and adaptive capacity at the neighborhood level.

2. DIMENSIONS OF NEIGHBORHOOD CLIMATE RESILIENCE

2.1. Urban Fabric and Its Role in Neighborhood Climate Resilience

This study examines the phenomenon of the urban heat island (UHI) within the context of urban climate risk. The concept entered the literature through the systematic demonstration that urban areas exhibit higher temperatures compared to their surrounding rural counterparts. In his work from 1833, Luke Howard provided one of the earliest accounts of the urban heat island phenomenon, showing that air temperatures in cities are generally higher than those in the surrounding rural areas (Oke, 1982). Today, the UHI is understood as a complex thermal anomaly—manifesting across horizontal, vertical, and temporal dimensions—that can be observed in a significant portion of both large and small-scale settlements. At the core of this phenomenon lie the alterations that urban development imposes on the energy balance of the natural or pre-urbanized surfaces upon

which a city is built (Stewart and Oke, 2012). Consequently, the urban heat island is not merely a meteorological phenomenon; it is an issue directly linked to patterns of urban development, land cover, and the physical characteristics of the built environment.

From the perspective of urban climate resilience, the relationship between the physical attributes of the built environment and the urban heat island constitutes a vital area of research for understanding the vulnerability of cities to climatic risks. The literature indicates that large cities, particularly those with high population density, are more susceptible to the urban heat island effect (Balaban, 2012). However, treating urban density alone as a negative determinant is insufficient. Compact urban forms that are mixed-use and pedestrian-friendly can contribute to mitigating the impacts of climate change by reducing energy consumption and greenhouse gas emissions resulting from transportation (Knuth et al., 2020). Therefore, it is not merely density that is decisive for the urban climate, but rather the qualities of the urban fabric and the spatial arrangement through which this density is manifested. In this context, the physical components of the urban fabric play a direct role in the formation and intensity of the urban heat island effect. The prevalence of impervious surfaces alters the energy and water balance of these surfaces, thereby intensifying the urban heat island effect (Ronchi et al., 2020). Similarly, the use of materials with low albedo leads to greater absorption of solar radiation, which exacerbates urban warming (Van Der Hoeven and Wandl, 2015). Furthermore, the form and geometric characteristics of buildings are also critical in shaping urban thermal conditions. The "urban canyon" effect—which emerges as building heights increase—influences atmospheric conditions and the spatial distribution of heat, contributing to heat accumulation in urban areas (Stanganelli and Soravia, 2012). Narrow streets and dense development reduce the sky view factor (SVF), which increases shading during the day while restricting the release of stored heat back into the atmosphere at night (Van Der Hoeven and Wandl, 2015). In parallel with this, the openness ratio at the street level and building density are considered urban morphological variables directly related to the formation of urban heat islands, as they influence the degree of shading and the continuity of airflow (Ramyar et al., 2019).

Land Surface Temperature (LST) is considered a key parameter for assessing the relationship between urban fabric and microclimatic conditions, as it reflects the capacity of the built environment to store and re-emit solar energy. It has been demonstrated that an increase in the building footprint ratio raises surface temperatures. However, a study conducted in Istanbul revealed that horizontal density (building footprint ratio) has a stronger influence on LST variations compared to vertical density (floor area ratio) (Erdem Okumuş and Terzi, 2022). Similarly, in a study examining the urban fabric characteristics that affect the Urban Heat Island (UHI) effect, the most significant variables were identified—in order of importance—as building density, building height, and the building footprint ratio (He et al., 2023).

On the other hand, the climatic resilience of the urban fabric cannot be explained solely by the density and geometric properties of buildings; the presence and continuity of natural and semi-natural components within the urban system also play a decisive role. In particular, the existence of large, integrated green spaces stands out as a fundamental urban feature for lowering surface temperatures (Ronchi et al., 2020). Furthermore, it has been noted that increasing tree cover in a neighborhood by 6% contributes to a reduction in the UHI effect (Kalaycı Kadak, 2025). The creation of water and green corridors within the urban fabric strengthens the connection between natural and built environments, thereby contributing to the promotion of air circulation (Arslan and Gençel, 2023; Ingaramo and Negrello, 2024). Similarly, biophilic design practices—such as green roofs, vertical greening, and roadside tree planting—are recognized as significant intervention tools for mitigating the Urban Heat Island (UHI) effect (Zhao et al., 2011; Newman, 2020).

These findings indicate that assessing urban climate resilience requires a comprehensive examination of the various morphological, spatial, and surface characteristics of the urban

fabric. Accordingly, this study employs a set of quantifiable indicators—representing different dimensions of the urban fabric—to evaluate its role in urban heat risk and climate resilience at the neighborhood scale. These indicators are defined as follows: (1) average parcel size, representing building characteristics at the parcel scale; (2) the Floor Area Ratio (FAR) and (3) the Building Coverage Ratio (BCR), which denote horizontal and vertical building density; (4) the street openness ratio, which reveals the spatial relationship between streets and buildings; (5) fractal dimensions, which assess the spatial complexity of the urban fabric; (6) the land cover ratio, representing the distribution of natural versus built surfaces; (7) the permeable surface ratio; and (8) the street network integration value, which indicates the level of spatial accessibility and integration within the street network.

The identified indicators represent various dimensions of the urban fabric and allow for a more detailed assessment of spatial characteristics related to urban heat risk and climate resilience. In this context, average parcel size reflects the parcel structure and spatial scale of the urban fabric, while the floor area ratio (FAR) and building coverage ratio (BCR) (He et al., 2023) indicate the total development density and the horizontal footprint of the structures. The street openness ratio (Ramyar et al., 2019) defines the geometric relationship between building masses and street voids, contributing to the evaluation of urban climate conditions—such as shading, solar exposure, and airflow. Fractal dimension and lacunarity (a measure of "gappiness") are used to assess the formal complexity, spatial organization, and degree of compactness of the urban fabric. The land cover ratio (Stanganelli and Spravia, 2012) and the permeable surface ratio (Ronchi et al., 2020) reveal the distribution of natural and semi-natural surfaces—key components of the urban climate system—within the urban fabric, thereby supporting the evaluation of surface characteristics in relation to the urban climate. Finally, the street network integration value (Tumturk et al., 2022) represents the relative position of streets within the urban network and their topological relationships with other streets. Spatial integration serves as a fundamental criterion for analyzing the accessibility and connectivity of streets within an urban network, thereby contributing to the assessment of the network structure of urban space. Considering these indicators allows for an assessment that goes beyond a mere focus on building density, thereby facilitating a comparative evaluation of the relationships between urban heat risk and climate resilience across neighborhoods.

2.2. Socio-economic Capacity and Neighborhood Climate Resilience

Physical events are defined as hazards when they have the potential to produce negative consequences for human well-being and safety. However, whether a hazard leads to such negative outcomes depends not only on the nature of the event itself but also on the characteristics of the elements exposed to it and their capacity to cope with its impacts. In this context, "exposure" refers to the presence of people, structures, infrastructure, and environmental elements—which could be affected by a given hazard—within the hazard-prone area. "Vulnerability," on the other hand, refers to the susceptibility of these elements to being negatively affected, encompassing their sensitivities, weaknesses, and limitations in coping capacity (Lavell et al., 2012; Oke et al., 2017). Social groups such as the elderly, children, or women as inherently "vulnerable" without considering their specific contextual circumstances risks overlooking the structural and societal factors that shape vulnerability. Vulnerability is not merely a condition explainable by individual or demographic traits; rather, it is a multidimensional process shaped by the interplay of historical, social, economic, political, cultural, and institutional conditions, as well as factors related to natural resources and the environment (Lavell et al., 2012). Consequently, social and spatial groups exposed to the same physical hazard may experience varying levels of damage and loss, depending on the resources they possess, the conditions in which they find themselves, and their capacity to cope (Cardona et al., 2012; Lavell et al., 2012). Structural factors—such as poverty, limited social networks, and inadequate access to social support mechanisms—shape the level and consequences of vulnerability, regardless of the specific hazard involved.

In understanding vulnerability and climate-related risks, the capacity to mobilize existing resources in the face of adverse impacts and to respond to changing conditions is also significant. Adaptive capacity refers to a system's ability to mitigate the negative effects of a given hazard and to respond to changing circumstances (Walker et al., 2004; Gallopin, 2006), playing a decisive role in risk reduction. Limited adaptive capacity can increase a system's vulnerability by restricting its ability to cope with the impacts of hazards and adapt to changing conditions (Chapagain et al., 2025). From a planning perspective, adaptive capacity is critical for enabling cities to manage both gradual environmental shifts and sudden, profound transformations. Accordingly, strengthening adaptive capacity through planning processes is essential for reducing vulnerability, supporting the continuity of ecosystem services, and mitigating the adverse effects of climate change (Eraydin, 2013). Therefore, when assessing the climate resilience of neighborhoods, it is necessary to consider both socio-economic conditions and the adaptive capacity shaped by those conditions.

The relevant literature indicates that a society's resilience to climate-related hazards is closely linked to its socio-economic conditions and adaptive capacity. Some studies show that household vulnerability is associated not only with exposure to hazards or inherent sensitivity but also with deficiencies in adaptive capacity (Rathi et al., 2021). At the national level, per capita income is considered a key indicator of adaptive capacity (Adger, 2001; Rathi et al., 2021). This is primarily because income relates to the ability of households and individuals to implement protective measures, improve housing conditions, and access necessary resources. However, evaluating socio-economic capacity solely based on income levels is insufficient for explaining the climate resilience of neighborhoods. The capacity of individuals and households to face climate-related risks, cope with their impacts, and adapt to changing conditions is shaped by a multitude of interrelated factors, including demographic structure, economic resources, education levels, and housing market conditions (Balaban, 2012; IPCC, 2022). Therefore, in this study, socio-economic capacity is addressed as a multidimensional construct, represented by measurable indicators that capture the social and economic disparities between neighborhoods. In this context, a total of six indicators were used: (1) population density (Técher et al., 2023), (2) average income level, (3) average market value (for sale and rent) in the neighborhood, (4) proportion of the vulnerable population (individuals aged 0–4 and over 65), (5) proportion of the population that is illiterate or has no formal education, and (6) proportion of the population with a university degree or higher.

Low levels of education, unemployment, and the lack of property ownership are socio-economic conditions that can increase vulnerability by restricting individuals' access to—and their capacity to implement—protective measures, such as insurance or housing improvements (Balaban, 2012; Button et al., 2013; Mohtat & Khirfan, 2022). Consequently, when assessing the capacity to cope with and adapt to climate risks, it is necessary to consider not only economic resources but also factors such as education and housing market conditions, which determine individuals' access to information and their ability to utilize available resources. Education level serves as an indicator of social vulnerability, influencing access to information, risk perception, participation in decision-making processes, and the development of protective behaviors. The average market value (for sale and rent) in a neighborhood reflects the economic value of the housing market and socio-economic differentiation between neighborhoods; it also provides insight into access to housing for different income groups and highlights spatial inequalities. Similarly, the "vulnerable population ratio"—defined as the share of children aged 0–4 and individuals aged 65 and older within the total population—has been used to assess the social vulnerability of neighborhoods. These age groups may exhibit a higher physiological sensitivity to the health impacts of climate-related hazards, such as extreme temperatures. Consequently, the proportion of these groups within the population serves as a significant social indicator, explaining why neighborhoods exposed to similar physical environmental conditions may experience varying levels of impact from temperature-related risks. Finally, population density reveals the spatial distribution of the population at the neighborhood

scale, thereby contributing to the assessment of the number of people potentially exposed to temperature hazards (Técher et al., 2023).

3. MATERIALS AND METHOD

3.1. Classification of Indicators

The comparison of neighborhoods falling within the same Local Climate Zone (LCZ) 2 class, in terms of urban heat resilience, was conducted based on three fundamental dimensions widely used in the literature: exposure, sensitivity, and adaptive capacity. In the IPCC's Fifth Assessment Report, risk is defined as the outcome of the interaction between a system's exposure, sensitivity, and adaptive capacity in the face of climate-related hazards (IPCC, 2014). Drawing upon this conceptual framework, the measurable indicators—identified through a review of the literature and constituting the study's dataset—were classified into these three dimensions (exposure, sensitivity, and adaptive capacity) based on their relationship to urban heat resilience. This framework also serves as the foundation for urban heat resilience indices used to assess urban heat and resilience at the neighborhood level (NHRI).

In this study, the indicators used to calculate urban heat resilience at the neighborhood scale were categorized into three primary groups—climatic and environmental indicators, socio-economic indicators, and urban fabric indicators—and subsequently organized under the dimensions of exposure, sensitivity, and adaptive capacity, according to their expected impact on resilience. This classification is based on the conceptual distinction between the degree to which a neighborhood is exposed to a climatic hazard, the characteristics that determine the extent to which its population is affected by that hazard, and the resources available to cope with or adapt to the hazard. The indicators were determined by considering physical and socio-economic characteristics associated in the literature with exposure, sensitivity, and adaptive capacity.

Exposure refers to the extent to which neighborhoods are subjected to the hazard of urban heat, as well as the physical and spatial conditions that influence this level. In this context, Land Surface Temperature (LST) was used as the primary exposure indicator, as it directly represents thermal conditions. Furthermore, indicators such as average parcel size, floor area ratio (FAR), building coverage ratio (BCR), street openness, street network integration, fractal dimension, and lacunarity (a measure of "gappiness" or void space) were examined under this dimension to assess how the geometric and spatial characteristics of the urban fabric relate to thermal exposure.

Sensitivity refers to demographic and socio-economic characteristics that may exacerbate the potential adverse effects of the urban heat hazard on the population. Within this dimension, population density was evaluated as an indicator representing the spatial concentration of people potentially affected by the heat hazard. Per capita income reflects disparities in the economic resources of households, while the proportion of vulnerable population represents the share of age groups—such as the elderly or very young—that may be particularly susceptible to the health impacts of extreme temperatures. These three indicators were used to assess how demographic and economic variations among neighborhoods relate to their sensitivity to urban heat.

Adaptive capacity refers to the social, economic, and environmental resources that neighborhoods possess to mitigate the adverse effects associated with urban heat, cope with these impacts, and adapt to changing conditions. In this context, the proportion of the population with no formal education and the proportion with a university degree or higher are considered social indicators related to access to information and the capacity to cope with risks. Property values (fair market values) as determined by the municipality serve as an indicator of economic resources at the neighborhood scale; meanwhile, the ratio of permeable surfaces, land cover, and Normalized Difference Vegetation Index (NDVI) are included under this dimension, as they contribute to thermal regulation and provide environmental resources for adaptation.

Online Journal of Art and Design
volume 15, issue 1, January 2027
DOI: https://doi.org/10.30935/ojad/2513146

Accordingly, land surface temperature (LST)—classified under the climate group—and seven urban fabric indicators constitute the exposure category. Three socio-economic indicators form the sensitivity category, while a combination of three socio-economic indicators and three urban fabric indicators makes up the components of adaptive capacity. Thus, the indicators employed in this study are structured to provide a holistic assessment of the thermal conditions in neighborhoods, the potential level of impact on the population, and the social, economic, and environmental resources available to mitigate such impacts. The classification reflects the conceptual framework adopted in this study, as well as the availability of indicators at the neighborhood scale. It is acknowledged that certain socio-economic and urban fabric indicators may relate to multiple dimensions. Therefore, their assignment should be understood within the context of their primary analytical roles in the proposed framework, rather than as mutually exclusive relationships. The classification of these indicators according to resilience components, along with their respective data sources, is presented in Table 1.

Table 1. Indicators, Data Sources, and Normalization Methods Used in the Calculation of the NHRI

Type	**Indicator**	**Resilience component**	**Data/Method used**	**Normalization type**
Climate and environmental indicators	Land surface temperature (LST)	Exposure	Landsat 8 / QGIS	Inverse
Socio-economic indıcators	Population density	Sensitivity	Endeksa	Inverse
	Average income level	Sensitivity	Endeksa	Linear
	Average fair market value (for sale and rent)	Adaptive capacity	Endeksa	Linear
	Vulnerable population rate (ages 0–4, 65+)	Sensitivity	Endeksa	Inverse
	Proportion of the population that is illiterate or uneducated	Adaptive capacity	Endeksa	Inverse
	Proportion of the population with a university degree or higher education	Adaptive capacity	Endeksa	Linear
Urban fabric indicators	Land cover ratio (built environment / green space)	Adaptive capacity	Google Earth/ GIS	Linear
	Permeable surface ratio	Adaptive capacity	Google Earth/ GIS	Linear
	Average parcel size	Exposure	TKGM.gov	Linear
	Street network integration value	Exposure	DepthmapX	Linear
	Fractal complexity value (D)	Exposure	Image J	Inverse
	Fractal lacunarity value (L)	Exposure	Image J	Linear
	Building Coverage Ratio (BCR)	Exposure	Google Earth/ GIS	Inverse
	Floor Area Ratio (FAR)	Exposure	Google Earth/ GIS	Inverse
	Normalized difference vegetation index (NDVI)	Adaptive capacity	Landsat 8/ QGIS	Linear
	Street aspect ratio (height / width)	Exposure	Google Earth/ GIS	Linear

3.2. Measurement of Neighborhood-Scale Heat Resilience

Although indicators may conceptually relate to multiple dimensions, each indicator has been scored and calculated to provide a consistent basis for assessing exposure, sensitivity, and adaptive capacity at the neighborhood level within its respective dimension. To calculate resilience scores for neighborhoods in relation to land surface temperature, all indicators were normalized on a scale of 0–1, based on their relationship with resilience (Table 1). Inverse normalization was applied to indicators that reduce resilience, while linear normalization was applied to those that enhance it. For indicators supported by the literature as contributing positively to resilience—such as income level, the proportion of the educated population, and the ratio of permeable surfaces—by reducing exposure and increasing adaptive capacity, the following approach was employed:

$$N_i = \frac{x_i - x_{\min}}{x_{\max} - x_{\min}}$$

Online Journal of Art and Design
volume 15, issue 1, January 2027
DOI: https://doi.org/10.30935/ojad/2513146

For indicators such as land surface temperature, the proportion of the population with low levels of formal education, the proportion of vulnerable populations, and building coverage and floor area ratios (BCR and FAR)—all of which increase sensitivity, diminish adaptive capacity, and heighten exposure, thereby negatively affecting urban heat island resilience:

$$N_i = \frac{x_{\max} - x_i}{x_{\max} - x_{\min}}$$

the following formulas have been used. Here:
•N_i: the normalized indicator value,
•x_i: the indicator value for the respective neighborhood,
•$x_{\min}$: the minimum value of the indicator,
•$x_{\max}$: the maximum value of the indicator.

To ensure a consistent interpretation across the three dimensions of resilience, all indicator scores were directionally standardized before being aggregated. Since high levels of exposure and sensitivity represent less favourable conditions, these dimensions were inversely normalized so that higher scores would indicate lower exposure and lower sensitivity. In contrast, adaptive capacity was normalized in its original direction, such that higher values represent greater adaptive capacity. Consequently, all three dimension scores can be interpreted in the same way: lower scores signify less favourable conditions, while higher scores signify more favourable conditions. The composite score for each dimension was calculated by taking the arithmetic mean of the normalized indicators pertaining to that dimension. In the final step, the neighborhood resilience score was calculated by taking the arithmetic mean of the three dimension scores, with equal weight assigned to each dimension.

$$NHRI_i = \frac{E_i + S_i + AC_i}{3}$$

•$NHRIi$ = the neighborhood's resilience score
•Ei = the directed exposure score
•Si = the directed sensitivity score
•ACi = the adaptive capacity score

A high NHRI value indicates that a neighborhood possesses a greater level of resilience against urban heat risks. This approach is based on the premise that, within urban systems, exposure to high temperatures and social vulnerability increase heat risk, whereas a high adaptive capacity serves to mitigate this risk. The resulting resilience score ranges from 0 to 1, with higher values representing a more favourable neighborhood resilience profile. The NHRI values are categorized into five classes: 0.80–1.00 (highly resilient), 0.60–0.79 (resilient), 0.40–0.59 (moderate), 0.20–0.39 (at-risk), and 0.00–0.19 (highly at-risk). This classification enables the determination of the relative standing of neighborhoods in terms of urban heat resilience and facilitates the comparison of neighborhoods with varying levels of resilience based on their urban fabric and socio-economic characteristics.

3.3. Socio-economic Capacity Classification and Sample Selection

To identify the sample areas for comparison in this study, a total of 93 neighborhoods located across three central districts of Konya were classified into three categories—low, medium, and high—based on their socio-economic capacity levels. This classification utilized 2025 demographic data from the Turkish Statistical Institute (TÜİK) and index data from April 2026, both provided by Endeksa. The socio-economic capacity levels of the neighborhoods were determined by considering several indicators: population density (persons/km²); the proportions of children aged 0–4 and the population aged 65+; education levels (ranging from illiterate and literate without formal schooling to primary, secondary, university, and postgraduate education); the distribution of socio-economic status (SES) classes (A+, A, B, C, and D); per capita income; and the price per square

Online Journal of Art and Design
volume 15, issue 1, January 2027
DOI: https://doi.org/10.30935/ojad/2513146

meter for both rental and for-sale housing. The socio-economic status classifications provided by Endeksa are generated through statistical models that utilize data on the active age group, real estate land values, residential rental and sale prices, household size, number of workplaces, number of ATMs and bank branches, the distribution of spending habits, and the elderly population.

The indicators obtained for the 93 neighborhoods were divided into three categories—low, medium, and high—based on the minimum, maximum, and mean values observed across the neighborhoods. Each category was assigned a score reflecting its level of resilience. For each indicator, a score of 2 was assigned to the category representing greater resilience (or lower vulnerability), 1 point to the category representing a medium level, and 0 points to the category representing greater disadvantage (or higher vulnerability). For instance, a high level of education or high income—which signify greater adaptive capacity—received 2 points, whereas high population density and a high proportion of vulnerable population segments—which increase vulnerability—received 0 points (Table 2).

To evaluate the distribution of socio-economic status classes at the neighborhood level, a weighted scoring system was applied: coefficients of 1, 2, 3, 4, and 5 were assigned to classes D, C, B, A, and A+, respectively, to calculate a weighted socio-economic status score for each neighborhood. Specifically, the proportions of each socio-economic status class within a given neighborhood were multiplied by their corresponding coefficients to derive an overall socio-economic status score for that neighborhood. In this way, the contribution of various socio-economic status groups to the general capacity level of each neighborhood was assessed through a single, unified score.

Table 2. Indicators and scoring system used in the socio-economic capacity classification of neighborhoods

Type	Data Used	Scoring
Demographics	Population density (persons/km²)	Low: 2, Medium: 1, High:0
	Total population of children aged 0–4 and individuals aged 65+	Low: 2, Medium: 1, High:0
	Number of illiterate individuals or those who are literate but have no formal education	Low: 2, Medium: 1, High:0
	Number of individuals with a university degree or higher	Low: 0, Medium: 1, High: 2
	Proportion of socio-economic status classes	Low: 0, Medium: 1, High: 2
	Per capita income (TRY)	Low: 0, Medium: 1, High: 2
Index	Price per m² for rental housing (April 2026)	Low: 0, Medium: 1, High: 2
	Price per m² for housing for sale (April 2026)	Low: 0, Medium: 1, High: 2

Following the scoring of all indicators, total scores were calculated for 93 neighborhoods, which were then categorized into three groups based on their socio-economic capacity: low (1–5 points), medium (6–10 points), and high (11–16 points). This classification was performed to ensure that the selected study areas would represent varying levels of socio-economic capacity. Subsequently, comparable study areas—all falling within the same LCZ 2 (Local Climate Zone 2) class—were identified to represent each socio-economic capacity group.

In selecting these study areas, the criteria included a predominantly built-up urban fabric, a primary function of residential use, the absence of boundaries adjacent to water bodies or forested areas, and a spatial extent of approximately 40,000 m². These criteria have been applied to ensure that the study areas remain consistent with the general physical characteristics of the LCZ 2 class, thereby allowing for comparisons to be made under the most similar physical conditions possible.

3.4. Urban Fabric Assessment

To assess the heat resilience of neighborhoods, the following urban fabric characteristics were used as indicators: average parcel size, building footprint ratio (TAKS), floor area ratio (KAKS), street aspect ratio, fractal dimension (D), void ratio (L), land cover ratio,

permeable surface ratio, street network integration value, and NDVI. Various data sources and analytical tools were employed to calculate these indicators, including the General Directorate of Land Registry and Cadastre (TKGM) Parcel Inquiry Application, Google Earth Pro, Netcad, DepthmapX, ImageJ, and QGIS.

Data regarding parcel boundaries and areas were obtained via the TKGM Parcel Inquiry Application (General Directorate of Land Registry and Cadastre, n.d.), and the average parcel size was calculated for each selected neighborhood. The TAKS and KAKS ratios were determined using total parcel areas from the TKGM Parcel Inquiry Application in conjunction with satellite and street-level imagery (dated February 16, 2026) accessed via Google Earth Pro. Street aspect ratios were calculated by dividing the average height of buildings fronting a street by the width of that street.

Fractal analysis is a method used to quantitatively evaluate the self-similarity—across different scales—and the spatial organization of irregular geometric structures. In this study, fractal dimensions were calculated using the "box-counting" method. For this analysis, urban fabric samples extracted from Google Earth satellite imagery were processed in Adobe Photoshop and converted into binary images, where building masses are represented in black and open spaces in white. The acquired images were saved in PNG format and analyzed using the FracLac plugin for the ImageJ software. For the fractal dimension calculations, the default box-counting scales of FracLac (2, 3, 4, 6, 8, 16, 32, and 64 pixels) were employed. The resulting D (fractal dimension) value represents the spatial complexity of the urban fabric and its capacity to fill space. In two-dimensional analyses, the D value theoretically ranges between 1 and 2. A D value approaching 1 indicates a pattern characterized by more discrete, regular, and low-density structures, whereas a value approaching 2 signifies a denser, more compact, and complex urban configuration. In general, D values <1.30 denote a low level of complexity, values in the 1.30–1.50 range indicate moderate complexity, and D values >1.50 signify high spatial complexity and dense urban development (Chen, 2020). Lacunarity (L)—a metric that complements the fractal dimension—reveals the distribution of voids within the urban fabric and the degree of spatial heterogeneity. Low lacunarity values point to more homogeneous and regular spatial patterns, while high values indicate a fragmented, heterogeneous urban structure characterized by an irregular distribution of voids (ImageJ, n.d.).

To calculate land cover and the ratio of permeable surfaces, the areas of permeable and impermeable surfaces were digitized using a Google satellite image dated February 16, 2026, within the Netcad software. Street network configuration is an approach that allows for the evaluation of the topological relationships of individual street segments within a network, as well as their spatial connections to other street segments. In this context, a space syntax analysis—conducted using the DepthmapX software—is employed to calculate various topological values for the street segments within the network. The "integration" value represents the extent to which a given segment is close to all other street segments within the network (Tumturk et al., 2022). In this study, rather than performing a comprehensive analysis of general walkability and accessibility, the focus is placed on the level of street network integration within each selected urban fabric. To compare the internal spatial organization of these urban fabrics—which are of similar size, each covering approximately 40,000 m²—a global integration (Rn) analysis was performed, and the mean global integration values were calculated for each sample area. To facilitate this analysis, the centerlines of the streets in each area were drawn as polylines using the Netcad 8.5.2 GIS software and saved in .dxf format. The resulting street network data were then imported into the DepthmapX software. In the first stage, axial maps were created; subsequently, segment maps were generated from these, and an integration analysis was performed. Given that the study areas are similar in size, the mean values of global integration (Rn) were used to compare the street network configurations of the sampled urban fabrics.

Online Journal of Art and Design
volume 15, issue 1, January 2027
DOI: https://doi.org/10.30935/ojad/2513146

For the NDVI calculation, Band 4 (Red) and Band 5 (Near-Infrared – NIR) from Landsat 8 satellite imagery were utilized. The analyses were conducted within the QGIS 3.44 environment using the Raster Calculator tool, and the NDVI values were calculated using the following formula (U.S. Geological Survey, n.d.):

$$NDVI = \frac{B5 - B4}{B5 + B4}$$

The NDVI raster data obtained from the calculations was overlaid with the boundaries of nine urban fabric study areas, which were defined using Google Earth. Subsequently, the minimum, maximum, and mean NDVI values for each sample fabric were calculated in QGIS using the zonal statistics interface.

For the Land Surface Temperature (LST) analysis, satellite data obtained from the USGS (United States Geological Survey) EarthExplorer database were used as raw data. All available images from June, July, and August 2025 were examined; however, due to high cloud cover (more than 10%) in most, a Landsat 8 Collection 2 Level-2 Science Product image from August 11, 2025 (LC08_L2SP_177034_20250811_20250821_02_T1)—which featured minimal cloud cover (3%)—was selected for the study. The analyses were conducted using QGIS 3.44 software. The ST_B10 surface temperature layer, included within the Landsat Collection 2 Level-2 product suite, was utilized. This layer contains surface temperature information derived from satellite-measured thermal data that has undergone atmospheric correction. The ST_B10 raster data were converted into degrees Celsius using the QGIS Raster Calculator tool. This conversion process was performed in accordance with the following equation (US Geological Survey, 2024):

$$T = 0.00341802 \times ST_B10 + 149.0 - 273.1$$

The stages that constitute the methodology of the study conducted in this direction are summarized as follows (Figure 1).

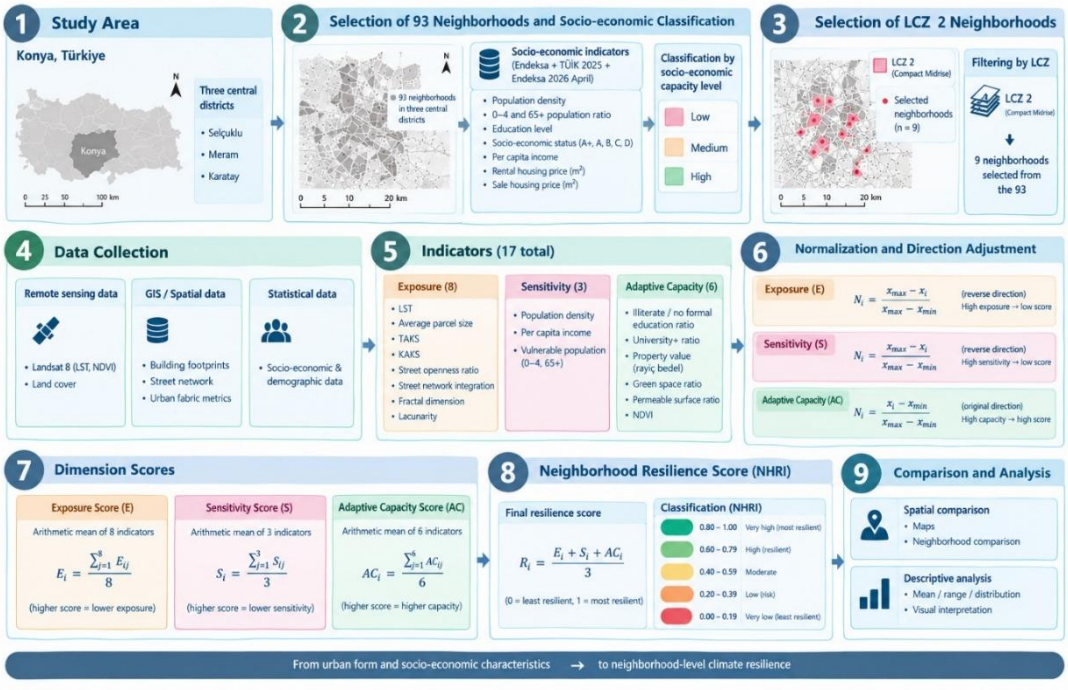


Figure 1. Methodological framework for assessing neighborhood climate resilience within LCZ 2.

Online Journal of Art and Design
volume 15, issue 1, January 2027
DOI: https://doi.org/10.30935/ojad/2513146

4. CASE STUDY: LCZ 2 NEIGHBORHOODS IN KONYA CITY

Konya, selected as the study area, experiences high temperatures and intense solar radiation during the summer months due to its continental, semi-arid climate. With an annual solar radiation level of approximately 1,608 kWh/m² (MGM, 2024a), the city's low humidity, minimal cloud cover, and long sunshine duration (averaging 7.4 hours) create conditions conducive to the pronounced observation of the urban heat island effect (MGM, 2024b). According to the "Konya Local Climate Change Adaptation Strategy and Action Plan," which examines the city at the district level, exposure to heatwaves is classified as "very high" or "high" in the Selçuklu, Meram, and Karatay districts (Ballı Gözen et al., 2021). Furthermore, Konya's predominantly flat topography and limited elevation variance make it an ideal setting for comparative neighborhood-level analyses, as the influence of terrain on the microclimate remains relatively consistent across the area.

Given the limited latitudinal variation (0.27°)[1] across the central districts of Selçuklu, Meram, and Karatay, it is assumed that macro-scale solar exposure and topographical conditions are largely uniform throughout the study area. Consequently, it is posited that any variations in the urban heat island effect between neighborhoods are primarily attributable to differences in urban fabric, land cover, and socio-economic characteristics. Furthermore, the distinct spatial differentiation in income levels and urban fabric allows for an examination of how socio-economic conditions influence urban heat resilience at the neighborhood scale. Additionally, while the existing literature is dominated by studies conducted in large metropolitan areas, there is a relative scarcity of research focusing on medium-sized cities (Leal Filho et al., 2018)—a gap that further justifies the selection of Konya as the study area.

The visualization tool provided by the World Urban Database enables the characterization of the physical urban structure based on the Local Climate Zone (LCZ) classification scheme—a framework developed by Stewart and Oke (2012) to standardize observation and documentation methods in urban heat island studies (WUDAPT, n.d). Using the "LCZ Generator," the general distribution of local climate zones within the study area—Konya—was mapped via Google Earth (Demuzere et al., 2021). The resulting classification indicates the presence of LCZ 1, LCZ 2, LCZ 3, LCZ 4, LCZ 5, LCZ 6, and LCZ 9 categories across Konya's central districts: Selçuklu, Meram, and Karatay (Figure 2).

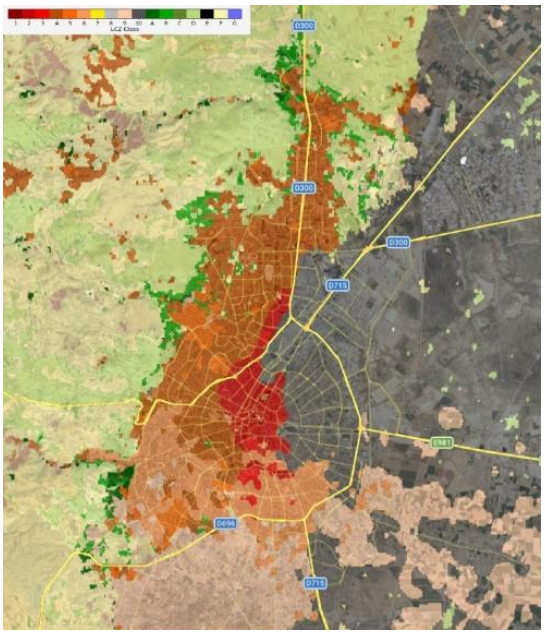


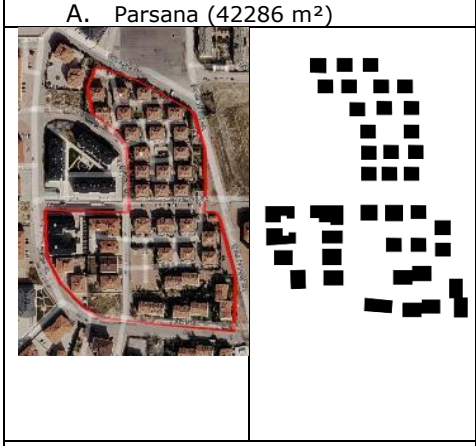
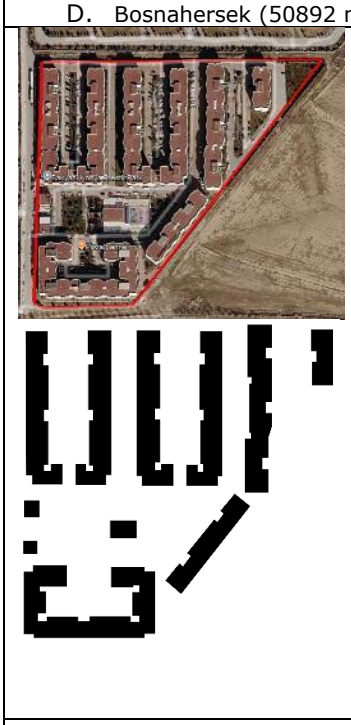
Figure 2: Classification of local climate zones in Konya (Derinci Alper, 2026)

[1] This difference corresponds to a change of well under 1% in the solar elevation angle.

Online Journal of Art and Design
volume 15, issue 1, January 2027
DOI: https://doi.org/10.30935/ojad/2513146

This study, a total of 9 urban fabrics—categorized under LCZ 2 (compact mid-rise development) and representing low, medium, and high socio-economic capacities (3 of each)—were examined. Sample areas, each covering approximately 40,000 m², were selected from the following neighborhoods: Parsana, Melikşah, and Havzan (high socio-economic capacity); Bosnahersek, Nişantaşı, and Konevi (medium socio-economic capacity); and Sahibata, Nakipoğlu, and Keçeciler (low socio-economic capacity). These urban fabrics are presented in Table 3.

Table 3: Selected urban fabrics and their characteristics (Google Earth and figure-ground plans)

A. Parsana (42286 m²)	B. Melikşah (36097 m²)	C. Havzan (38169 m²)
		
D. Bosnahersek (50892 m²)	E. Nişantaşı (45025 m²)	F. Konevi
		
G. Sahibata (46783 m²)	H. Nakipoğlu (35545 m²)	I. Keçeciler (40652 m²)

Online Journal of Art and Design
volume 15, issue 1, January 2027
DOI: https://doi.org/10.30935/ojad/2513146



5. FINDINGS

5.1. Findings of the socio-economic indicators

Based on demographic data provided by Endeksa—which utilizes 2025 data from the Turkish Statistical Institute (TÜİK)—the information presented in Table 4 has been analyzed at the neighborhood level (Endeksa, n.d.). An examination of population density across three distinct socio-economic capacity groups reveals a density of 8571 people/km² in neighborhoods within the high-capacity group, 12323 people/km² in the medium-capacity group, and 15947 people/km² in the low-capacity group. Regarding per capita income, the figures are 29038 TL for the high-capacity category, 25159 TL for the medium-capacity category, and 15086 TL for the low-capacity category. Consequently, it can be observed that as socio-economic capacity decreases, population density increases, while per capita income declines. In terms of household size and the proportion of the "vulnerable population"—defined here as children and the elderly—neighborhoods in the high socio-economic capacity category have an average household size of 3,28 and a vulnerable population ratio of 14,95%. For neighborhoods in the medium-capacity category, the average household size is 3,00 with a vulnerable population ratio of 17,51%, while for those in the low-capacity category, the average household size is 3,20 with a vulnerable population ratio of 16,70% (Table 4).

Table 4: Demographic and Index Data Examined in the Sample Areas

District	Neighborhood name	Population density people/km²	Per capita income (TRY)	Household size	Vulnerable population rate (%)	Illiterate or uneducated population rate (%)	Proportion of population with undergraduate or postgraduate degrees (%)	Average fair market value in the neighborhood (for rent) (TRY)	Average fair market value in the neighborhood (for sale) (TRY)
Selçuklu	Parsana	5008	25427	3,31	12,68	8,61	28	176	40772
Meram	Havzan	13825	30661	3,42	14,59	7,86	36	169	36381
Meram	Melikşah	6881	31025	3,11	17,57	7,41	33	156	31132
Average		8571	29038	3,28	14,95	7,96	32,33	167	36095
Selçuklu	Bosnahersek	6911	16901	3,26	11,08	7,03	19	144	23562
Selçuklu	Nişantaşı	18205	26076	2,89	20,54	7,64	30	140	21775
Meram	Konevi	11853	32499	2,87	20,92	7,75	33	157	20909
Average		12323	25159	3	17,51	7,47	27,33	147	22082
Meram	Sahibata	8177	16719	2,91	18,93	8,53	14	137	13177
Karatay	Keçeciler	21908	14862	3,33	16,19	9,17	13	142	21549
Karatay	Nakipoğlu	19971	13570	3,37	16,58	10,63	13	144	22731
Average		15947	15086	3,20	16,70	9,49	14	138,75	20258

When examining the educational attainment levels in the neighborhoods where the selected sample areas are located, it is observed that the proportion of the population that is illiterate or lacks formal education is quite similar between the medium (7,47%) and high (7,96%) socio-economic capacity groups, whereas it is higher in the low-capacity category (9,49%). Regarding the proportion of the population with undergraduate or postgraduate degrees, this figure is highest in the high socio-economic capacity group

Online Journal of Art and Design
volume 15, issue 1, January 2027
DOI: https://doi.org/10.30935/ojad/2513146

(32,33%), followed by 27,33% in the medium category, and only 14% in the neighborhoods within the low-capacity category. Finally, an analysis of the neighborhood-level average market values for rental and for-sale properties—based on index data provided by Endeksa—reveals that neighborhoods in the high socio-economic capacity group exhibit higher average values for both rentals and sales compared to the other groups; meanwhile, the average market values in the medium and low-capacity categories show a progressive decline corresponding to their respective categories.

5.2. Findings of the urban fabric indicators

In the earlier phase of the study, as presented in Table 3.1, variables classified according to the dimensions of exposure, sensitivity, and adaptive capacity were analyzed using various methods and employed to calculate a neighborhood resilience score. The findings obtained are shown in the table below (Table 5). Based on this table, the findings for each indicator—detailed in the subheadings below—were derived.

Table 5: Findings on Urban Fabric Indicators

Socio-economic capacity	District	Neighborhood name	Average parcel size (m²)	BCR	FAR	Street aspect ratio	Fractal values	Land cover ratio	Permeable surface ratio	Street network integration value	NDVI
High	Selçuklu	Parsana	4018	0,30	0,90	0,34	D:1,541 L: 0,3641	6	14	33,35	0,102
	Meram	Havzan	649	0,45	1,35	1,28	D: 1,6736 L: 0,3441	6	15	37,28	0,135
	Meram	Melikşah	1680	0,45	2,25	3,00	D: 1,6674 L: 0,3242	16	6	32,86	0,116
	Average		2116	0,4	1,5	1,54	D:1,6273 L:0,3441	9,3	11,6	34,50	0,118
Medium	Selçuklu	Bosnahersek	50892	0,30	1,50	0,80	D:1,6013 L: 0,3406	5	18	29,18	0,119
	Selçuklu	Nişantaşı	369	0,60	3,00	1,80	D:1,6992 L: 0,3356	6	14	39,37	0,122
	Meram	Konevi	421	0,55	2,20	1,70	D:1,7156 L: 0,2983	3	26	26,88	0,123
	Average		17227	0,57	2,6	1,75	D:1,6720 L:0,3248	4,6	19,3	31,81	0,12
Low	Meram	Sahibata	204	0,70	2,50	1,50	D:1,7216 L: 0,3193	5	17	48,45	0,109
	Karatay	Keçeciler	440	0,50	2,50	1,10	D: 1,6298 L: 0,3348	12	8	38,48	0,100
	Karatay	Nakipoğlu	1064	0,75	3,00	2,10	D:1,6944 L: 0,3036	4	20	42,39	0,098
	Average		569	0,63	2,8	1,29	D:1,6819 L:0,3119	7	15	43,11	0,10

5.2.1. Average parcel size

When examining the average parcel sizes for each group, the mean parcel size is 2116 m² for urban fabrics in the high category, 17227 m² for those in the medium category, and 569 m² for those in the low category.

5.2.2. Building coverage ratio, floor area ratio and street aspect ratio

For urban fabrics in the high category, the average building coverage ratio (BCR) is 0,4, the floor area ratio (FAR) is 1,5, and the street aspect ratio is 1,54. For those in the medium category, the average BCR is 0,57, the FAR is 2,6, and the street aspect ratio is 1,75. For fabrics in the low category, the average BCR is 0,63, the FAR is 2,8, and the street aspect ratio is 1,29. Accordingly, it can be stated that for the LCZ 2 category, as socio-economic capacity decreases, the building footprint size and total floor area within these urban fabrics increase, while there is very little variation in the street aspect ratios.

5.2.3. Fractal dimension

An examination of the average fractal values across all selected urban fabrics reveals similar values, characterized by high spatial complexity and dense development. Notably,

Online Journal of Art and Design
volume 15, issue 1, January 2027
DOI: https://doi.org/10.30935/ojad/2513146

the urban fabric selected from the Parsana neighborhood—which falls into the high socio-economic capacity group—exhibits the lowest complexity value, whereas the fabric selected from the Sahibata neighborhood—categorized within the low socio-economic capacity group—proves to be the most complex. Regarding the distribution of open spaces, the urban fabric selected from the Konevi neighborhood (in the medium socio-economic capacity group) displays a more homogeneous structure compared to the others; conversely, the fabric selected from the Parsana neighborhood (in the high socio-economic capacity group) possesses a more heterogeneous structure, with open spaces distributed in an irregular manner.

5.2.4. Land cover ratio and permeable surface ratio

Among the nine urban fabrics examined, the one selected from the Konevi neighborhood—which falls into the medium socio-economic capacity category—exhibited the lowest land cover ratio and the highest ratio of permeable surfaces. Conversely, the urban fabric selected from the Melikşah neighborhood—which belongs to the high socio-economic capacity group—displayed the highest land cover ratio and the lowest ratio of permeable surfaces. When analyzed by socio-economic capacity groups, neighborhoods in the medium category were found to have the lowest land cover ratio and the highest ratio of permeable surfaces, whereas the urban fabrics in neighborhoods with high socio-economic capacity exhibited the highest land cover ratio and the lowest ratio of permeable surfaces.

5.2.5. Street network configuration

An examination of the average integration values reveals that the selected urban fabrics with low socio-economic capacity exhibit the highest level of integration, with a value of 43,11. Conversely, the urban fabrics with medium socio-economic capacity show the lowest level of integration, with a value of 31,81. This indicates that, among the LCZ 2 urban fabrics analyzed, areas with low socio-economic capacity feature a more integrated and permeable street network structure.

5.2.6. NDVI

An examination of the analysis reveals that the mean NDVI values for the selected areas are quite close to one another, suggesting that they possess a similar density of vegetation cover.

5.3. Climate and environmental indicator (LST)

The temperature values—minimum, maximum, and average—derived from the analysis are presented in Table 6. Accordingly, the urban fabric with the highest surface temperature (43,56 ℃) is in the Parsana neighborhood, which belongs to the high socio-economic capacity group. The urban fabric with the lowest surface temperature (40,97 ℃) is found in the Melikşah neighborhood, which falls into the same category. When average surface temperature values are examined across high, medium, and low socio-economic capacity groups, it is observed that the urban fabrics in the high and medium categories exhibit temperatures 0,4 ℃ lower than those in the low socio-economic capacity group.

Table 6: LST Values of Selected Urban Fabrics (℃)

District	Neigborhood name	Minimum	Maksimum	Average
Selçuklu	Parsana	42,38	45,42	43,56
Meram	Havzan	40,86	42,31	41,56
Meram	Melikşah	40,31	41,60	40,97
Average		41,18	43,11	42,3
Selçuklu	Bosnahersek	41,33	46,33	43,07
Selçuklu	Nişantaşı	40,36	42,49	41,65
Meram	Konevi	40,13	42,03	41,39
Average		40,60	43,62	42,04

Online Journal of Art and Design
volume 15, issue 1, January 2027
DOI: https://doi.org/10.30935/ojad/2513146

Meram	Sahibata	40,78	42,56	41,89
Karatay	Keçeciler	42,11	43,56	42,63
Karatay	Nakipoğlu	42,32	43,31	42,84
Average		41,74	43,15	42,45

5.4. Findings on the dimensions of neighborhood climate resilience

When examining the average neighborhood exposure scores, the selected urban fabrics in the high socio-economic capacity group show an average of 0,58, while those in the medium and low categories show averages of 0,41 and 0,34, respectively (Table 7). Accordingly, it can be stated that, among the areas examined, urban fabrics in the high socio-economic category are less exposed to the Urban Heat Island (UHI) effect. The area with the highest exposure score is an urban fabric located in the Parsana neighborhood (0,66), while the area with the lowest exposure is an urban fabric selected from the Nakipoğlu neighborhood, which falls into the low socio-economic capacity group (0,26).

Table 7: Neighborhood Exposure Scores

General Information		Exposure*								
Neighborhood name	Socio-economic capacity	LST score	Average parcel size score	BCR score	FAR score	Street aspect ratio score	Street network configuration score	Fractal dimension (D) score	Fractal dimension (L) score	Average exposure score
Parsana	High	0,00	1,00	1,00	1,00	0,00	0,30	1,00	1,00	0,66
Havzan	High	0,77	0,12	0,67	0,79	0,35	0,48	0,27	0,71	0,52
Melikşah	High	1,00	0,39	0,67	0,36	1,00	0,28	0,33	0,42	0,55
Average										0,58
Bosnahersek	Medium	0,19	1,00	1,00	0,71	0,17	0,11	0,66	0,71	0,57
Nişantaşı	Medium	0,74	0,06	0,33	0,00	0,55	0,58	0,16	0,57	0,37
Konevi	Medium	0,84	0,04	0,44	0,38	0,51	0,00	0,05	0,00	0,28
Average										0,41
Sahibata	Low	0,64	0,00	0,11	0,24	0,44	1,00	0,00	0,28	0,34
Keçeciler	Low	0,36	0,23	0,56	0,24	0,29	0,54	0,55	0,57	0,42
Nakipoğlu	Low	0,28	0,06	0,00	0,00	0,66	0,75	0,16	0,14	0,26
Average										0,34

*Lower average exposure scores indicate that the areas have a higher level of exposure.

When examining the average neighborhood sensitivity scores across socio-economic capacity groups, the values are 0,73 for areas in the high-capacity category, 0,50 for those in the medium-capacity category, and 0,25 for those in the low-capacity category (Table 8). The area with the highest sensitivity score (0,82) is a specific urban fabric located in the Parsana neighborhood—which falls into the high socio-economic capacity group—while the areas with the lowest average sensitivity scores (0,18) are found in the Keçeciler and Nakipoğlu neighborhoods, both of which belong to the low-capacity category. As shown in Table 8, sensitivity score increases as socio-economic capacity decreases.

Table 8: Neighborhood Sensitivity Scores

General Information		Sensitivity*			
Neighborhood name	Socio-economic capacity	Population density score	Per capita income score	Vulnerable population score	Average Vulnerability Score
Parsana	High	1,00	0,62	0,83	0,82
Havzan	High	0,47	0,90	0,64	0,67
Melikşah	High	0,88	0,92	0,34	0,71
Average					0,73
Bosnahersek	Medium	0,88	0,17	1,00	0,68

Online Journal of Art and Design
volume 15, issue 1, January 2027
DOI: https://doi.org/10.30935/ojad/2513146

Nişantaşı	Medium	0,21	0,66	0,03	0,30
Konevi	Medium	0,59	1,00	0,00	0,53
Average					0,53
Sahibata	Low	0,81	0,16	0,20	0,39
Keçeciler	Low	0,00	0,06	0,48	0,18
Nakipoğlu	Low	0,11	0,00	0,44	0,18
Average					0,25

*Lower average sensitivity scores indicate that the areas possess a higher degree of sensitivity.

When examining the mean adaptive capacity scores, the average for urban fabrics in the high category is 0,63, for those in the medium category it is 0,50, and for those in the low category it is 0,22 (Table 9). The urban fabric selected in the Havzan neighborhood—which falls into the high category—possesses the highest adaptive capacity with a score of 0,73, while the urban fabric in the Nakipoğlu neighborhood—which belongs to the low socio-economic capacity group—has the lowest adaptive capacity with a score of 0,18. Based on these findings, it can be concluded that adaptive capacity decreases as socio-economic capacity declines.

Table 9: Neighborhood Adaptive Capacity Scores

General information		Adaptive capacity							
Neighborhood name	Socio-economic capacity	Illiterate and uneducated population score	Population with under-graduate and postgraduate education score	Average market value in the neigh. score (for rent)	Average market value in the neigh. score (for sale)	Land cover ratio score	Permeable surface ratio score	NDVI score	Average score for adaptive capacity
Parsana	High	0,56	0,65	1,00	1,00	0,23	0,40	0,00	0,55
Havzan	High	0,76	1,00	0,82	0,84	0,23	0,45	1,00	0,73
Melikşah	High	0,89	0,86	0,48	0,65	1,00	0,00	0,33	0,60
Average									0,63
Bosnahersek	Medium	1,00	0,26	0,17	0,37	0,15	0,60	0,66	0,46
Nişantaşı	Medium	0,83	0,73	0,07	0,31	0,23	0,40	0,66	0,46
Konevi	Medium	0,80	0,86	0,51	0,28	0,00	1,00	0,66	0,59
Average									0,50
Sahibata	Low	0,58	0,04	0,00	0,00	0,15	0,55	0,33	0,24
Keçeciler	Low	0,40	0,00	0,12	0,30	0,69	0,10	0,00	0,23
Nakipoğlu	Low	0,00	0,00	0,17	0,34	0,07	0,70	0,00	0,18
Average									0,22

Neighborhood Heat Resilience Scores were generated by calculating the arithmetic mean of the exposure, sensitivity, and adaptive capacity values (Table 10). Based on the results, the neighborhoods of Parsana (0,68), Havzan (0,64), and Melikşah (0,62)—which fall into the high socio-economic capacity group—are classified as "resilient." Meanwhile, the neighborhoods of Bosnahersek (0,57) and Konevi (0,47) fall into the "moderately resilient" category, and the area selected from the Nişantaşı neighborhood (0,38) is classified as "low resilience." Within the low socio-economic capacity group, the neighborhoods of Sahibata (0,32), Keçeciler (0,28), and Nakipoğlu (0,21) are categorized as having low resilience.

Online Journal of Art and Design
volume 15, issue 1, January 2027
DOI: https://doi.org/10.30935/ojad/2513146

Table 10: Neighborhood Heat Resilience Scores

General information		Neighborhood heat resilience score	Neighborhood heat resilience score
Neighborhood name	Socio-economic capacity		
Parsana	High	0,68	Resilient
Havzan	High	0,64	Resilient
Melikşah	High	0,62	Resilient
Bosnahersek	Medium	0,57	Moderate
Nişantaşı	Medium	0,38	At Risk
Konevi	Medium	0,47	Moderate
Sahibata	Low	0,32	At Risk
Keçeciler	Low	0,28	At Risk
Nakipoğlu	Low	0,21	At Risk

An examination of the findings regarding exposure, sensitivity, and adaptive capacity reveals that the results for exposure underscore the significance of urban fabric characteristics in assessing heat exposure. Nakipoğlu Neighborhood, which falls into the low socio-economic capacity group, exhibits the highest exposure value (0,26), whereas Parsana Neighborhood, belonging to the high-capacity group, shows the lowest exposure value (0,66). In Nakipoğlu, alongside high Land Surface Temperature (LST), one observes smaller parcel sizes, higher BCR and FAR, and a more integrated street network; in contrast, Parsana is characterized by larger parcels and lower BCR and FAR values. The fact that total exposure in Parsana is low—despite a high LST—demonstrates that heat exposure at the neighborhood scale should not be evaluated solely based on LST and highlights the importance of considering urban fabric indicators in conjunction.

Regarding the sensitivity dimension, Nakipoğlu and Keçeciler (0,18) emerge as the most sensitive neighborhoods, while Parsana (0,82) presents the lowest sensitivity value. The higher sensitivity observed in Nakipoğlu and Keçeciler—driven by high population density and low per capita income—indicates that socio-economic conditions must be considered when assessing the vulnerability profiles of neighborhoods to climatic risks. Conversely, Parsana's low population density, smaller proportion of vulnerable population, and higher income level are associated with a lower sensitivity profile.

Findings regarding adaptive capacity reveal that even neighborhoods within the same Local Climate Zone (LCZ 2) category can exhibit substantial differences in terms of their socio-economic and environmental assets. Nakipoğlu possesses the lowest adaptive capacity (0.18), whereas Havzan possesses the highest (0.73). In Nakipoğlu, factors such as low education levels, a high proportion of the population lacking formal education, limited green space, and a high density of built-up areas converge; conversely, in Havzan, higher education levels, greater land values, and an abundance of green space are associated with a higher adaptive capacity. These findings demonstrate that socio-economic resources and environmental assets can lead to significant disparities in the potential for neighborhoods to remain resilient against climate-related risks. Specifically, neighborhoods with higher education levels and greater economic resources can be expected to have a stronger capacity to adapt to climate-driven risks, while those with lower socio-economic capacity and limited green space may exhibit a lower adaptive capacity. Such inequalities highlight that climate-related risks are not solely dependent on environmental conditions; rather, a neighborhood's existing social and economic resources also influence its capacity to withstand these risks. From the perspective of climate justice, this situation underscores the need to provide greater support to neighborhoods with lower socio-economic capacity.

6. DISCUSSION AND CONCLUSION

This study reveals that neighborhoods classified within the same Local Climate Zone (LCZ 2) can exhibit variations in terms of urban heat resilience. A comparative analysis of nine neighborhoods in Konya—all falling under the LCZ 2 category—demonstrates that urban fabric characteristics, socio-economic conditions, and environmental amenities collectively shape a neighborhood's potential for heat resilience. The findings indicate that while the LCZ classification provides an analytical framework for comparing urban fabrics based on their morphological and physical attributes, belonging to the same LCZ class does not imply that neighborhoods possess similar levels of heat exposure, sensitivity, or adaptive capacity. In this regard, the study shows that urban heat resilience cannot be explained solely through built-form patterns or land surface temperatures; rather, it requires multidimensional approaches that simultaneously account for the physical, social, economic, and environmental characteristics of neighborhoods.

When evaluated across all dimensions of resilience, it becomes evident that a neighborhood's urban heat resilience is linked not merely to the individual levels of exposure, sensitivity, or adaptive capacity, but to the specific combination of these dimensions. Neighborhoods characterized by low socio-economic capacity—compounded by high sensitivity and limited environmental amenities—may exhibit a disadvantageous resilience profile against climate-related risks. This underscores the fact that urban heat resilience is not merely a matter of physical or technical planning; The distribution of resources is also linked to social inequalities and access to environmental amenities. Analyzing neighborhoods within the same LCZ class has made it possible to examine physical, social, and economic differences between neighborhoods while keeping the general built-environment typology relatively constant. The findings indicate that the LCZ classification alone is insufficient to explain variations in resilience at the neighborhood scale and that this classification must be supplemented with socio-economic and environmental indicators.

From a planning perspective, the findings indicate that interventions addressing urban heat should not be applied uniformly across all neighborhoods; rather, they should be tailored to the specific exposure, sensitivity, and adaptive capacity profile of each neighborhood. In neighborhoods such as Nişantaşı, Sahibata, Keçeciler, and Nakipoğlu—which exhibit moderate to low resilience—strategies could include increasing permeable surfaces, creating shaded areas, expanding green spaces, and designing open spaces in alignment with local climatic conditions. Interventions concerning building density should not focus solely on reduction; they must also account for street geometry, shading, ventilation, and the quality of open spaces. Furthermore, mechanisms that support low-income households in improving their dwellings, social support for vulnerable groups, and initiatives that enhance access to information regarding climate risks should be integrated with physical environmental interventions. Consequently, urban heat resilience should be addressed through a holistic planning approach that considers not only environmental adjustments but also social and economic inequalities.

There are several limitations to consider when interpreting the results of this study. Due to the limited number of study areas, the analysis is primarily descriptive and comparative in nature, rather than statistically generalizable. Future studies utilizing larger sample groups, diverse LCZ categories, and data from various time periods could provide a more comprehensive assessment of neighborhood climate resilience. Furthermore, it would be possible to conduct a more comprehensive assessment by utilizing a larger dataset of surface temperatures recorded under suitable conditions. In the study, only a single temperature map was used, as there was no data available with low cloud-cover levels for the specified time period. It is also feasible to carry out a cross-sectional analysis using surface temperature data obtained from different dates. Incorporating more detailed socio-economic and environmental information could further broaden the understanding of neighborhood heat resilience. Consequently, policies focused on climate change adaptation and resilience against urban heat must account for variations at the neighborhood scale,

prioritizing areas that exhibit high vulnerability and limited adaptive capacity. Such an approach could not only help mitigate urban heat risks but also address inequalities in access to environmental amenities, fostering a more equitable planning paradigm aligned with the principles of climate justice.

References

Adger, W. N. (2001). Scales of governance and environmental justice for adaptation and mitigation of climate change. *Journal of International development*, *13*(7), 921-931.

Anguelovski, I., Shi, L., Chu, E., Gallagher, D., Goh, K., Lamb, Z., ... & Teicher, H. (2016). Equity impacts of urban land use planning for climate adaptation: Critical perspectives from the global north and south. *Journal of Planning Education and Research*, *36*(3), 333-348.

Arslan, F., & Gençel, Z. (2023). Ekolojik Akıllı Kent Bağlamında Kentsel Dokular. *Sketch: Journal of City and Regional Planning*, *4*(01-02), 1-23.

Balaban, O. (2012). Climate change and cities: a review on the impacts and policy responses. *METU Journal of Architecture* (29:1) 21-44.

Ballı Gözen, C., Demir, M. E., Dursun D., Aydın L., Babalık, E., Evci Kiraz, E.D., Karapınar, B., Kepenek Bozkırlıoğlu, A. Ö., Özdemir, A. D., Talu, N., Tolunay, D. ve Toy, S. (2021). Konya İli Etkilenebilirlik ve Risk Analizi Raporu. Türkiye'de İklim Değişikliğine Uyum Eyleminin Güçlendirilmesi Projesi. Birleşmiş Milletler Kalkınma Programı. T.C. Çevre Şehircilik ve İklim Değişikliği Bakanlığı. https://iklimeuyum.org/wp-content/uploads/2023/08/Konya_Etkilenebilirlik_Risk_Analizi.pdf

Button, C., Mias-Mamonong, M. A. A., Barth, B., & Rigg, J. (2013). Vulnerability and resilience to climate change in Sorsogon City, the Philippines: learning from an ordinary city?. *Local environment*, *18*(6), 705-722.

Cardona, O.D., M.K. van Aalst, J. Birkmann, M. Fordham, G. McGregor, R. Perez, R.S. Pulwarty, E.L.F. Schipper, and B.T. Sinh, (2012). Determinants of risk: exposure and vulnerability. In: Managing the Risks of Extreme Events and Disasters to Advance Climate Change Adaptation [Field, C.B., V. Barros, T.F. Stocker, D. Qin, D.J. Dokken, K.L. Ebi, M.D. Mastrandrea, K.J. Mach, G.-K. Plattner, S.K. Allen, M. Tignor, and P.M. Midgley (eds.)]. A Special Report of Working Groups I and II of the Intergovernmental Panel on Climate Change (IPCC). Cambridge University Press, Cambridge, UK, and New York, NY, USA, pp. 65-108.

Chapagain, P. S., Banskota, T. R., Shrestha, S., Khanal, N. R., Yili, Z., Yan, J., ... & Poudel, K. R. (2025). Studies on adaptive capacity to climate change: a synthesis of changing concepts, dimensions, and indicators. *Humanities and Social Sciences Communications*, *12*(1), 1-10.

Chen, Y. (2020). Fractal modeling and fractal dimension description of urban morphology. *Entropy, 22*(9), 961. https://doi.org/10.3390/e22090961

Derinci Alper, Gizem (2026). WUDAPT Level 0 training data for Konya (Turkey, Republic of), submitted to the LCZ Generator. This dataset is licensed under CC BY-NC-SA, and more information is available at https://lcz-generator.rub.de/factsheets/7518cd55a8005010d7e0df296a01e8ecc6169333/7518cd55a8005010d7e0df296a01e8ecc6169333_factsheet.html

Eraydin, A. (2013). Resilience Thinking for Planning. *In Resilience thinking in urban planning*. Dordrecht: Springer, 17-37.

Eraydin, A. and Taşan-Kok, T. (2013). Introduction: Resilience Thinking in Urban Planning. In *Resilience Thinking in Urban Planning*, 1–16.

Erdem Okumus, D., & Terzi, F. (2021). Evaluating the role of urban fabric on surface urban heat island: The case of Istanbul. *Sustainable Cities and Society*, *73*, 103128.

Erdem Okumus, D., & Terzi, F. (2022). Reconsidering Urban Densification for Microclimatic Improvement: Planning and Design Strategies for Istanbul. *ICONARP International Journal of Architecture and Planning*, 10 (2), 660-687. DOI: 10.15320/ICONARP.2022.220

Gallopín, G. C. (2006). Linkages between vulnerability, resilience, and adaptive capacity. *Global environmental change*, *16*(3), 293-303.

He, T., Zhou, R., Ma, Q., Li, C., Liu, D., Fang, X., Yina, H. & Gao, J. (2023). Quantifying the effects of urban development intensity on the surface urban heat island across building climate zones. *Applied Geography*, *158*, 103052.

Ingaramo, R., & Negrello, M. (2024). Strategies for adapting the dense Italian cities to the climate change. *TeMA-Journal of Land Use, Mobility and Environment*, 115-136.

IPCC, (2014). Climate Change 2014: Synthesis Report. Contribution of Working Groups I, II and III to the Fifth Assessment Report of the Intergovernmental Panel on Climate Change (R.K. Pachauri and L.A. Meyer (eds.)). IPCC, Geneva, Switzerland.

IPCC, (2022). Key risks across sectors and regions. In H.-O. Pörtner et al. (Eds.), *Climate change 2022: Impacts, adaptation and vulnerability*. Cambridge University Press. https://doi.org/10.1017/9781009325844.016

Kalaycı Kadak, M. (2025). Towards a climate-resilient metropolis: A neighborhood-scale nature-based urban adaptation planning approach. *Sustainability*, *17*(16), 7356.

Kennedy, C., Pincetl, S., & Bunje, P. (2011). The study of urban metabolism and its applications to urban planning and design. *Environmental pollution*, *159*(8-9), 1965-1973.

Knuth, S., Stehlin, J., & Millington, N. (2020). Rethinking climate futures through urban fabrics:(De) growth, densification, and the politics of scale. *Urban Geography*, *41*(10), 1335-1343.

Lavell, A., M. Oppenheimer, C. Diop, J. Hess, R. Lempert, J. Li, R. Muir-Wood, ve Myeong, S. (2012). Climate change: new dimensions in disaster risk, exposure, vulnerability, and resilience. In: Managing the Risks of Extreme Events and Disasters to Advance Climate Change Adaptation [Field, C.B., V. Barros, T.F. Stocker, D. Qin, D.J. Dokken, K.L. Ebi, M.D. Mastrandrea, K.J. Mach, G.-K. Plattner, S.K. Allen, M. Tignor, and P.M. Midgley (eds.)]. A Special Report of Working Groups I and II of the Intergovernmental Panel on Climate Change (IPCC). Cambridge University Press, Cambridge, UK, and New York, NY, USA, pp. 25-64.

Leal Filho, W., Icaza, L. E., Neht, A., Klavins, M., & Morgan, E. A. (2018). Coping with the impacts of urban heat islands. A literature based study on understanding urban heat vulnerability and the need for resilience in cities in a global climate change context. *Journal of Cleaner Production*, *171*, 1140-1149.

MGM, (2024a). Türkiye Yıllık Güneş Radyasyonu. https://www.mgm.gov.tr/FILES/resmi-istatistikler/parametreAnalizi/2024-gunes-radyasyonu.pdf

MGM, (2024b). Türkiye Günlük Güneşlenme Süreleri. https://www.mgm.gov.tr/FILES/resmi-istatistikler/parametreAnalizi/2024-guneslenme-sureleri.pdf

Mohtat, N., & Khirfan, L. (2022). Distributive justice and urban form adaptation to flooding risks: spatial analysis to identify Toronto's priority neighborhoods. *Frontiers in sustainable cities*, *4*, 919724.

Newman, P. (2020). Cool planning: How urban planning can mainstream responses to climate change. *Cities*, *103*, 102651.

Oke, T. R. (1982). The energetic basis of the urban heat island. *Quarterly journal of the royal meteorological society*, *108*(455), 1-24.

Oke, T. R., Mills, G., Christen, A., & Voogt, J. A. (2017). *Urban climates*. Cambridge university press.

Rahmani, N., & Sharifi, A. (2025). Urban heat dynamics in Local Climate Zones (LCZs): A systematic review. *Building and Environment*, *267*, 112225.

Ramyar, R., Ramyar, A., Kialashaki, Y., Bryant, M., & Ramyar, H. (2019). Exploring reconfiguration scenarios of high-density urban neighborhoods on urban temperature–The case of Tehran (Iran). *Urban Forestry & Urban Greening*, *44*, 126398.

Rathi, S. K., Chakraborty, S., Mishra, S. K., Dutta, A., & Nanda, L. (2021). A heat vulnerability index: Spatial patterns of exposure, sensitivity and adaptive capacity

for urbanites of four cities of India. *International journal of environmental research and public health*, *19*(1), 283.

Ronchi, S., Salata, S., & Arcidiacono, A. (2020). Which urban design parameters provide climate-proof cities? An application of the Urban Cooling InVEST Model in the city of Milan comparing historical planning morphologies. *Sustainable Cities and Society*, *63*, 102459.

Stanganelli, M., & Soravia, M. (2012). Connections between urban structure and urban heat island generation: An analysis trough remote sensing and GIS. In *Computational Science and Its Applications–ICCSA 2012: 12th International Conference, Salvador de Bahia, Brazil, June 18-21, 2012, Proceedings, Part II 12* (pp. 599-608). Springer Berlin Heidelberg.

Stewart, I. D. (2024). Origins and evolution of the local climate zone classification. In *Local Climate Zone Application in Sustainable Urban Development: Experience from East and Southeast Asian High-Density Cities* (pp. 19-33). Cham: Springer International Publishing.

Stewart, I. D., & Oke, T. R. (2012). Local climate zones for urban temperature studies. *Bulletin of the American Meteorological Society*, *93*(12), 1879-1900.

Técher, M., Ait Haddou, H., & Aguejdad, R. (2023). Urban heat island's vulnerability assessment by integrating urban planning policies: A case study of Montpellier Méditerranée metropolitan area, France. *Sustainability*, *15*(3), 1820.

Timmeren, V. A. (2012). Climate Integrated Design and Closing Cycles Solutions for a Sustainable 'Urban Metabolism'. In *Sustainable urban environments: An ecosystem approach* (pp. 313-339). Dordrecht: Springer Netherlands.

Tumturk, O., Karakiewicz, J., & De Haan, F. (2022). Adaptability of urban grids: patterns of morphological change and persistence in Midtown Manhattan, 1884-2011.

U.S. Geological Survey. (2024). *Landsat 8-9 Collection 2 Level 2 science product guide* (LSDS-1619, Version 6.0). https://d9-wret.s3.us-west-2.amazonaws.com/assets/palladium/production/s3fs-public/media/files/LSDS-1619_Landsat8-9-Collection2-Level2-Science-Product-Guide-v6.pdf

General Directorate of Land Registry and Cadastre. (n.d.). *Parsel sorgu*. https://parselsorgu.tkgm.gov.tr/

ImageJ. (n.d.). *What is lacunarity?* https://imagej.net/ij/plugins/fraclac/FLHelp/Lacunarity.htm

U.S. Geological Survey. (n.d.). Landsat normalized difference vegetation index. https://www.usgs.gov/landsat-missions/landsat-normalized-difference-vegetation-index

World Urban Database and Access Portal Tools (WUDAPT). (n.d.). *Local climate zones*. https://www.wudapt.org/lcz/

Demuzere, M., Kittner, J., Bechtel, B. (2021). LCZ Generator: a web application to create Local Climate Zone maps. Frontiers in Environmental Science 9:637455. https://doi.org/10.3389/fenvs.2021.637455

Endeksa. (n.d.). *Endeksa*. https://www.endeksa.com/tr/

Van Der Hoeven, F., & Wandl, A. (2015). Amsterwarm: Mapping the landuse, health and energy-efficiency implications of the Amsterdam urban heat island. *Building Services Engineering Research and Technology*, *36*(1), 67-88.

Walker, B., Holling, C. S., Carpenter, S. R. and Kinzig, A. (2004). Resilience, adaptability and transformability in social–ecological systems. *Ecology and society*, 9(2), 5.

Wang, R., Cai, M., Shi, Y., & Ren, C. (2024). Integration of LCZ to planning strategies. In *Local climate zone application in sustainable urban development: experience from East and Southeast Asian High-Density cities* (pp. 229-241). Cham: Springer International Publishing.

Wu, J., & Wu, T. (2013). Ecological resilience as a foundation for urban design and sustainability. In *Resilience in ecology and urban design: Linking theory and practice for sustainable cities* (pp. 211-229). Dordrecht: Springer Netherlands.

Zhao, C., Fu, G., Liu, X., & Fu, F. (2011). Urban planning indicators, morphology and climate indicators: A case study for a north-south transect of Beijing, China. *Building and Environment*, *46*(5), 1174-1183.